Hindawi Publishing Corporation
Journal of Nanoparticles
Volume 2013, Article ID 685836, 7 pages
http://dx.doi.org/10.1155/2013/685836

Research Article

Green Synthesis of Nanocrystalline Cu_2ZnSnS_4 Powder Using Hydrothermal Route

Shri kant Verma,[1] Vikash Agrawal,[1] Kiran Jain,[1] Renu Pasricha,[2] and Suresh Chand[1]

[1] *Organic and Hybrid Solar Cell Group, National Physical Laboratory (CSIR), New Delhi 110 012, India*
[2] *Material & Chemical Microscopy Group, National Physical Laboratory (CSIR), New Delhi 110 012, India*

Correspondence should be addressed to Kiran Jain; kiran@mail.nplindia.org

Received 12 April 2013; Accepted 7 May 2013

Academic Editor: Amir Kajbafvala

Nanocrystalline Cu_2ZnSnS_4 (CZTS) powder was synthesized by a hydrothermal process, using thiourea as sulfur precursor. The powder was qualitatively analyzed using X-ray to identify the phase, and the size of the particles was determined using transmission electron microscopy (TEM). Raman peak at 337.5 cm^{-1} confirms the formation of pure CZTS particles. The powder was also synthesized solvothermally using ethylenediamine as solvent. The hydrothermally synthesized powder indicated the presence of the kesterite phase Cu_2ZnSnS_4 and particle size of about 4-5 nm. This environmentally green synthesis by hydrothermal route can produce gram scale synthesis of material with a chemical yield in excess of ~ 90%. UV Vis absorption spectra measurements indicated the band gap of as-synthesized CZTS nanoparticles to be 1.7 eV, which is near the optimum value for photovoltaic solar cell, showing its possible use in photovoltaics.

1. Introduction

Thin film solar cells based on chalcopyrite type semiconductors like $CuInSe_2$, $CuInGaSe_2$ (CIGS), and so forth have shown high efficiency and applicability for large scale applications [1]. CIGS based solar cells exhibit improved stability under long-term excitation, and their best efficiency available nowadays exceeds 20% [2]; however, gallium and indium used for preparation of the active layer are rare earth elements and are expensive also. Hence, $Cu_2ZnSn(SSe)_4$ was found of more interest, because of less toxicity, earth abundance, nearly optimum direct band gap (E_g) of about 1.05–1.50 eV, and a high absorption coefficient [3, 4]. Compared with the vacuum approaches, the nonvacuum approaches are the more desired techniques to achieve low production costs, because of the advantages offered by these methods, such as simplicity, easy to scale up, and high material utilization [4, 5]. Diverse deposition routes of Cu_2ZnSnS_4 (CZTS) thin films such as sputtering, spray pyrolysis, sol-gel, and electro-deposition have been reported [6, 7]. Much attention has been focused recently on fabrication of low cost and highly efficient solar cells. In this respect, the synthesis of nanocrystalline powders through wet chemical routes is gaining importance, since spin casting or printing nanocrystalline powders enable roll to roll processing for large scale manufacturing. Solar cells based on $Cu_2ZnSnSe_4$ (CZTS) have achieved power conversion efficiencies as high as 11.1% using a hydrazine based approach [8]. However, hydrazine is highly toxic and very unstable, and its use requires extreme caution during handling. Recent advances in the synthesis of colloidal semiconductor nanocrystals (NCs) have paved the way for the use of a large variety of different techniques for the preparation of nanoparticle inks [9, 10]. Decreasing the particle size to the quantum confinement regime allows the band gap to be tuned as a function of the crystallite size, which facilitates the realization of multijunctions. Another advantage of using NCs is well controlled stoichiometry, which is one of the limiting steps of other deposition methods. To adapt these NCs for industrial purposes, in solar cell applications, the development of synthesis methods enabling the precise control of size, shape, and composition is of crucial importance. In the last few years, the synthesis of colloidal CZTS NCs appeared, and the use of CZTS inks for solar cell applications has also been demonstrated [9–14]. The choice of a user friendly method of large scale nanocrystalline synthesis process is a prerequisite to successively achieve the mission of cost effectiveness. There

are not many reports on the synthesis of nanocrystalline CZTS powders. Thin film solar cells based on colloidal route have achieved a power conversion efficiency of 7.3% and 8.4% [9, 10].

Hydrothermal/solvothermal process is an attractive route for large scale synthesis of nanocrystalline powders. Hydrothermal reactions have been widely used to synthesize nanocrystalline materials such as TiO_2, ZnO, CdS, ZnS, and ZnSe [11–18]. Ternary semiconductor quantum dots $CuInS_2$, $CuInSe_2$ have also been prepared by this method [19, 20]. Madarász et al. [21] prepared CZTS using thermal decomposition of thiourea complexes of Cu (I), Zn (II), and Sn (II) chlorides. Hydrothermal/solvothermal processing route was used to synthesize CZTS and related materials [22–29]. Wang et al. [22] synthesized CZTS by hydrothermal process. Cao and Shen [23] synthesized CZTS by solvothermal route, wherein ethylenediamine (EDA) was used as a solvent. Jiang et al. [24] reported the synthesis of orthorhombic CZTS using a hydrothermal method using EDA. In this approach, a mixed solvent EDA and water of 1 : 1 ratio and thiocarbamide were used as sulfur source. The presence of EDA and the annealing temperature were reported by Jiang et al. [24] to play an important role in the process of CZTS phase transitions between the tetragonal and orthorhombic structures. Large scale single crystalline CZTS nanosheets of thickness as thin as 20 nm were produced by a solvothermal approach depending on the EDA concentration [26].

In the present work, we have synthesized CZTS nanopowder by hydrothermal method, using thiourea as sulfur agent. This method is milder, simpler, more practical, and more ecofriendly than the solvothermal method, which uses EDA as solvent. The results demonstrate that hydrothermal route produces single phase nanocrystalline kesterite phase of CZTS. These investigations indicated that the formation of a crystal phase is closely related to the reaction conditions and the sulfur source, the solvent may affect the size and phase properties. The physical properties of the CZTS nanocrystalline particles, such as structure, morphology, and optical properties, were studied. The as-synthesized CZTS nanoparticles prepared in water showed a kesterite phase, with nanocrystallite size of 4-5 nm. The use of water as a solvent offers a more green or environmentally benign process, removing the requirement of organic solvents or hazardous substances. From the viewpoint of green chemistry, the hydrothermal approach is a good candidate since the reaction can proceed at a mild temperature in water in a sealed environment. Taking organic compound thiourea as a source of sulfur, the toxicity is lowered as compared with H_2S or Na_2S. Furthermore, thiourea decomposes at a temperature of about 80°C and releases S_2^- slowly, causing the reaction to proceed slowly and control easily.

2. Experimental

2.1. Synthesis of Nanocrystalline Cu_2ZnSnS_4 Powder. CZTS nanocrystalline powder was synthesized by solvothermal as well as hydrothermal route. In the solvothermal process, appropriate amounts of analytical grade $CuCl_2$, $(C_2H_3O_2)_2Zn$, $SnCl_4$, and S were added into a stainless steel autoclave with a teflon liner, which was filled with ethylenediamine up to 50% of the total volume (1000 mL). The autoclave was sealed and maintained at 180°C for 16 h and then allowed to cool to room temperature naturally. The precipitates were filtered off and washed with absolute ethanol. Finally, the product was collected for characterization.

In a hydrothermal process, appropriate amounts of analytical grade $CuCl_2$, $(C_2H_3O_2)_2Zn$, $SnCl_4$ and NH_2CSNH_2 (thiourea) were added into a stainless steel autoclave with a teflon liner, which was filled with double distilled water up to 50% of the total volume (1000 mL). The concentration of thiourea was kept 20% higher than stoichiometric ratio for the complete sulfurization of the compound. The autoclave was sealed and maintained at 180°C for 16 h and then allowed to cool to room temperature naturally. The precipitate was filtered off and washed with double distilled water.

2.2. Characterization. Structural characteristics of powders were determined by X-ray diffraction in 2θ range from 10° to 80° using Bruker Analytical X-ray diffractometer equipped with graphite-monochromatized Cu Kα radiation (λ = 1.5418 Å) and transmission electron microscope using a JEOL 2010F TEM operating at an accelerating voltage of 100 kV. For TEM measurements, carbon coated copper grids were prepared by dispersing 0.1 g powder in 10 ml deionized (DI) water by ultrasonic treatment for about 250 sec. One drop of this solution was placed over grid and left to dry. The particle size and morphology were investigated by UV Vis absorption spectra which were taken on a UV Vis spectrophotometer (Shimadzu UV-1601), in which chloroform was used as a reference solvent. Raman measurements were performed using Renishaw inVia Raman spectrometer, operating at 514.5 nm Ar ion laser.

3. Results and Discussion

Figure 1 shows the XRD pattern of the as-synthesized CZTS nanocrystalline particles. The diffraction pattern of the hydrothermally synthesized CZTS powder showed peaks at 2θ = 28.66, 33.1, 47.77, 56.70, 69.59, and 76.94°. All of these peaks can be indexed to the kesterite phase of CZTS (JCPDS 26-0575). The major XRD diffraction peaks can be attributed to the (112), (200), (220), and (312) planes, respectively. Similar peaks were present in the powder synthesized by solvothermal process.

Besides these results, some extra peaks at 2θ of 26.822, 30.811, and 51.891°, indicated by solvothermally prepared CZTS powder, can be attributed to the diffraction peaks of (100), (102), and (103) planes of wurtzite structure of ZnS (JCPDS36-1450). No direct information could be found to confirm the existence of SnS or SnS_2. An earlier report on solvothermal synthesis had shown similar impurity phase that was removed on annealing [23]. The powder prepared by hydrothermal route do not show presence of ZnS impurity phase. According to the Debye-Scherrer formula $d = 0.9\lambda/(\beta \cdot \cos\theta)$, where β is the line width at an angle 2θ and λ is X-ray wave length. The diameter d of both hydrothermal

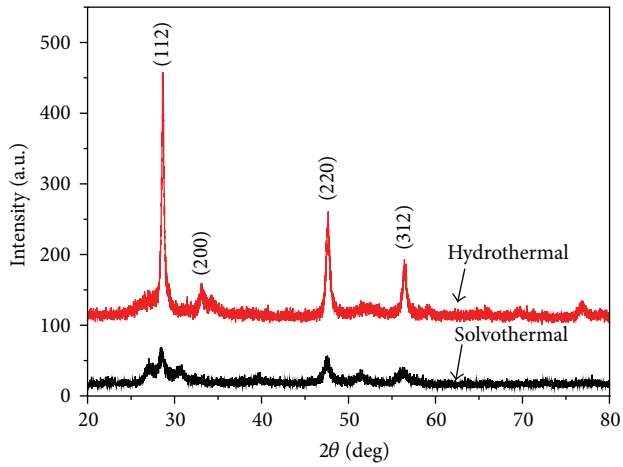

FIGURE 1: XRD pattern of as-synthesized CZTS powders.

and solvothermal synthesis routes of CZTS gives average nanoparticle size within 4-5 nm range.

As the XRD pattern of the CZTS particles is very similar to those of ZnS and Cu_2SnS_4, the Raman spectra of the material was used to characterize the final material. Figures 2(a) and 2(b) show the Raman scattering data for hydrothermally and solvothermally synthesized nanoparticles. Raman peaks for Cu_2S, ZnS, and SnS_2 are expected at 472 cm^{-1}, 351 cm^{-1}, and 315 cm^{-1}, respectively [30, 31]. In the present samples, the line widths are quite broad. The broadening of Raman peaks has been observed previously for nanocrystals of other materials and attributed to phonon confinement within the nanocrystals. This, together with the low intensity of the Raman peaks, made it very difficult to clearly identify the presence of impurity phases, especially in hydrothermally synthesized nanoparticles. For the material synthesized by hydrothermal route, Figure 2(a) showed a wide peak present at 335 cm^{-1}, and no other peak in the 100–500 cm^{-1} region was observed. On the other hand, the sample synthesized by solvothermal route showed three peaks present at 236, 343, and 472 cm^{-1}. The peaks present at 343, and 472 cm^{-1} may belong to the CZTS and Cu_2S phases, respectively. The presence of peaks other than that of CZTS further confirmed the presence of impurity phases in solvothermally synthesized material. Similar results were observed earlier by Cao and Shen, even though the impurity phases disappear after annealing [23]. On the other hand, in hydrothermal synthesis at 180°C, even the as-synthesized CZTS material is almost in pure phase, with negligible impurity phases.

Figures 3(a)–3(d) show the TEM image of hydrothermally synthesized CZTS nanoparticles. Figures 3(a) and 3(b) showed the presence of several small sized monodispersed CZTS nanoparticles of size 4 to 5 nm. Figure 3(b) shows the presence of sharper lattice fringes in the images of corresponding nanoparticles (encircled) that shows the high crystallinity of these nanoparticles. The selected area electron diffraction pattern of CZTS nanocrystals shown in Figure 3(c) confirms the single crystalline nature of nanoparticles. Also, the pattern matches well with JCPDS data card number 26-0575 as indicated by the diffraction rings corresponding to the (200) and (220) planes of the kesterite structure of CZTS nanoparticles. Figure 3(d) shows the enlarged view of nanoparticle encircled in Figure 3(b) and the lattice fringes in the high resolution TEM image are separated by 0.31 nm which matches the spacing distance of the (112) plane of Cu_2ZnSnS_4 nanocrystals.

Figures 4(a) and 4(d) show the transmission electron microscopic (TEM) image of CZTS nanoparticles synthesized by solvothermal method. Figures 4(a) and 4(c) show the CZTS nanoparticles of spherical shape having average size 5-6 nm. Figure 4(b) showed the agglomerated cluster of CZTS nanoparticles of size ~100 nm, which consists of several small CZTS nanoparticles. Inset of Figure 4(a) displays the HRTEM image of CZTS nanoparticles that shows the lattice fringe distance of 0.31 nm belonging to the (112) plane of the kesterite structure. Figure 4(d) shows the SAED ring pattern of polycrystalline CZTS nanoparticles.

The absorption spectra were measured in chloroform and the as-prepared nanocrystals were ultrasonically dispersed for several minutes in chloroform. Final solution was then transferred to the cuvette to measure the absorption spectra, and pure chloroform was used as reference. Figure 5(a) shows absorption spectra of CZTS nanoparticles, synthesized by hydrothermal and solvothermal methods. The band gaps were obtained by plotting $(Ah\nu)^2$ as a function of $h\nu$. Hydrothermally synthesized powder shows an optical band gap of 1.7 eV, while the solvothermally synthesized powder showed a band gap of 1.5 eV. This value corresponds well with the literature values and is near the optimum value for photovoltaic solar conversion in a single-band-gap device. The energy band structure of CZTS has already been calculated, and the measured band gap of kesterite CZTS is within 1.4–1.5 eV [20, 21], and since the crystallite size of CZTS powder for hydrothermally synthesized powder is near 4-5 nm, some band gap enhancement is expected due to quantum confinement.

The chemical composition of nanocrystals was determined using XRF technique. The composition obtained for solvothermal route showed the presence of molar concentration of different components as (Cu = 2, Zn = 0.7, Sn = 1.07, and S = 3.57) with lesser Zn; however, for hydrothermal route, the composition is slightly deficient in Cu as compared to Zn and Sn (Cu = 2, Zn = 1.23, Sn = 1.45, and S = 4.11). These compositions were calculated on average area of sample since large area of the thin film of CZTS was scanned. These relative chemical compositions were obtained for a film of 1 inch × 1 inch dimension, and thus, a large number of particles have been simultaneously analyzed. Therefore, they represent an average value.

The synthesis of large scale nanopowders by green technology is gaining importance nowadays. In this respect, the present hydrothermal synthesis of CZTS powder is important since water is a nonpolluting and nontoxic medium to synthesize nanopowders. Also, in hydrothermal process, reaction takes place in a closed reactor; thus, no fumes/gases are released in the atmosphere. The hydrothermally synthesized CZTS nanoparticles exhibited a good solubility in the isopropanol and showed a black color due to their strong

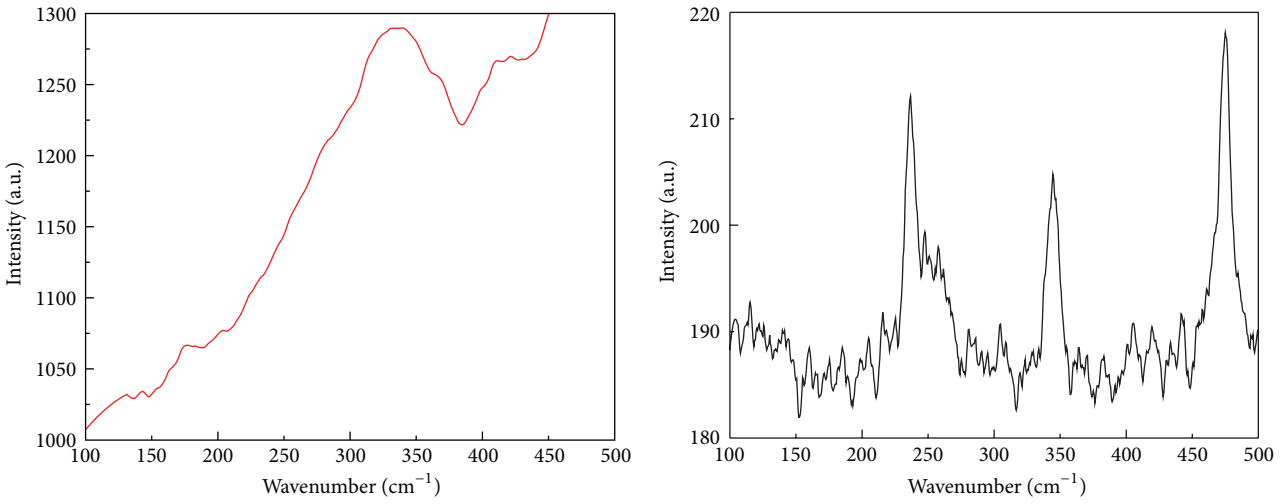

Figure 2: Raman spectra for CZTS nanoparticles synthesized by (a) hydrothermal and (b) solvothermal route.

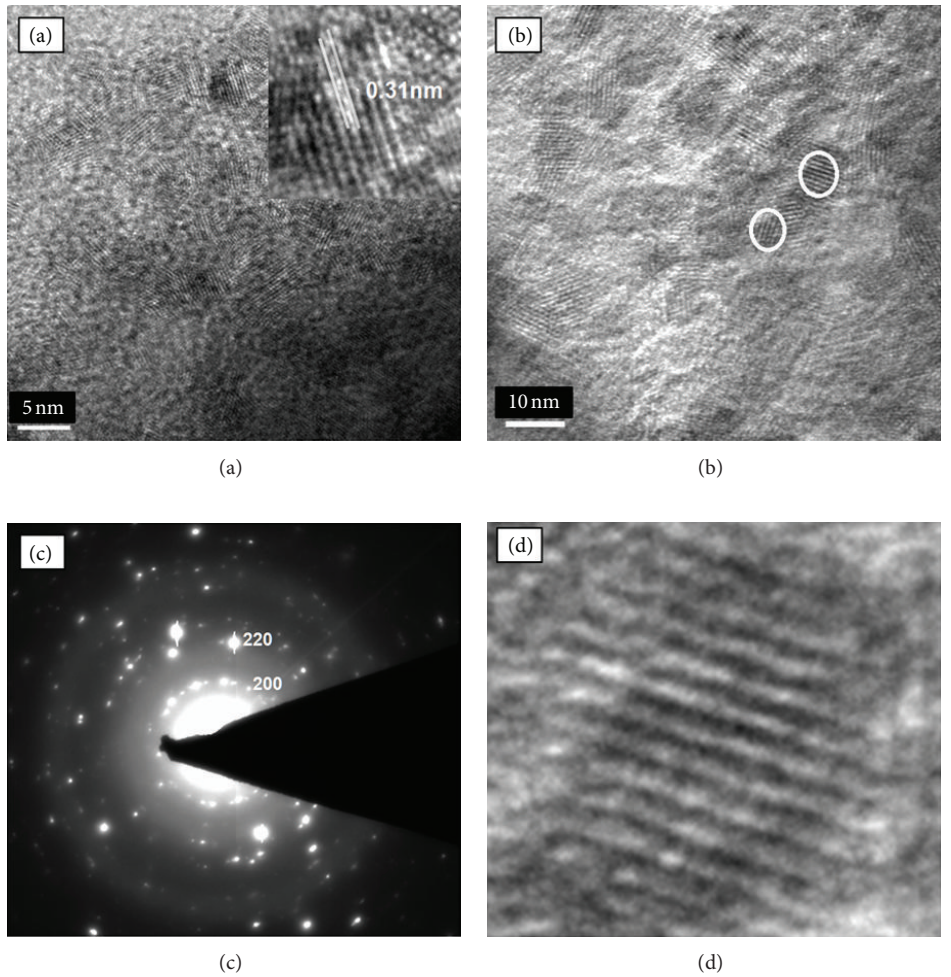

Figure 3: TEM images of hydrothermally synthesized CZTS powder: (a) average particle size (inset lattice fringes), (b) average particle size, (c) electron diffraction pattern, and (d) lattice fringes in single particle.

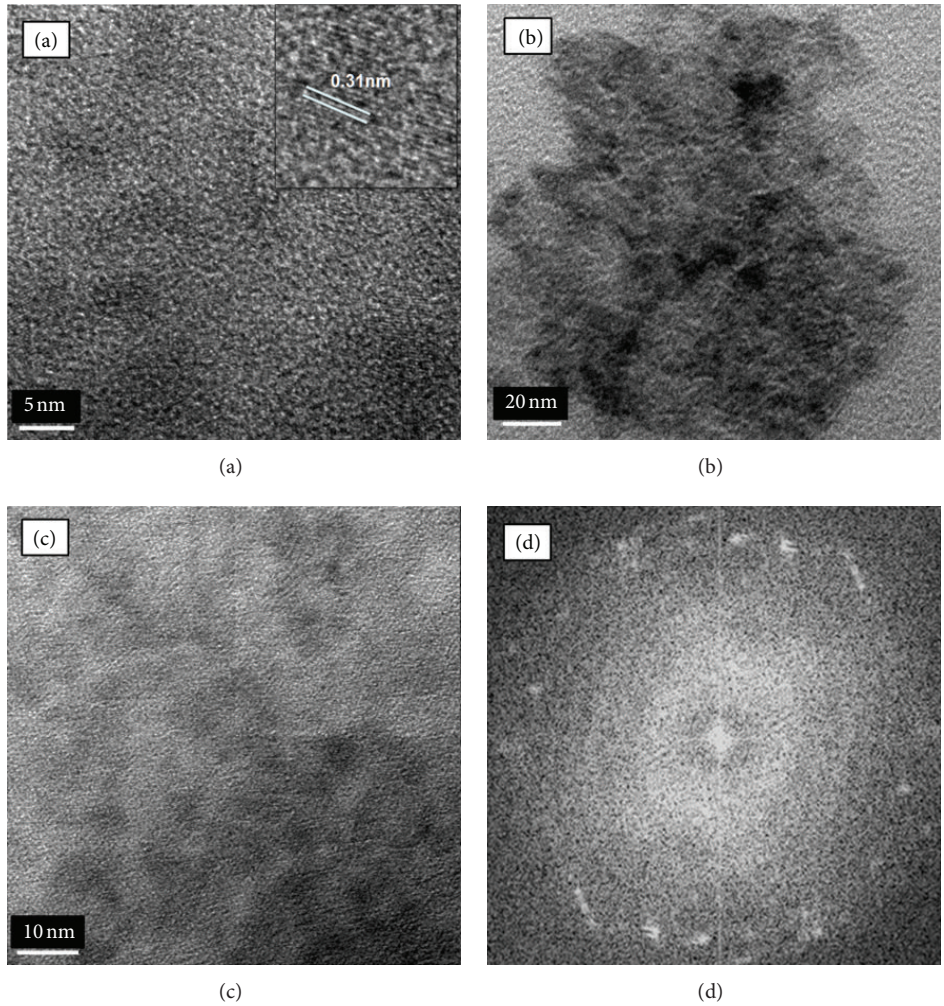

FIGURE 4: TEM images of solvothermally synthesized CZTS powder: (a) average particle size (inset lattice fringes), (b) cluster of nanoparticles, (c) distributed nanoparticles, and (d) electron diffraction pattern.

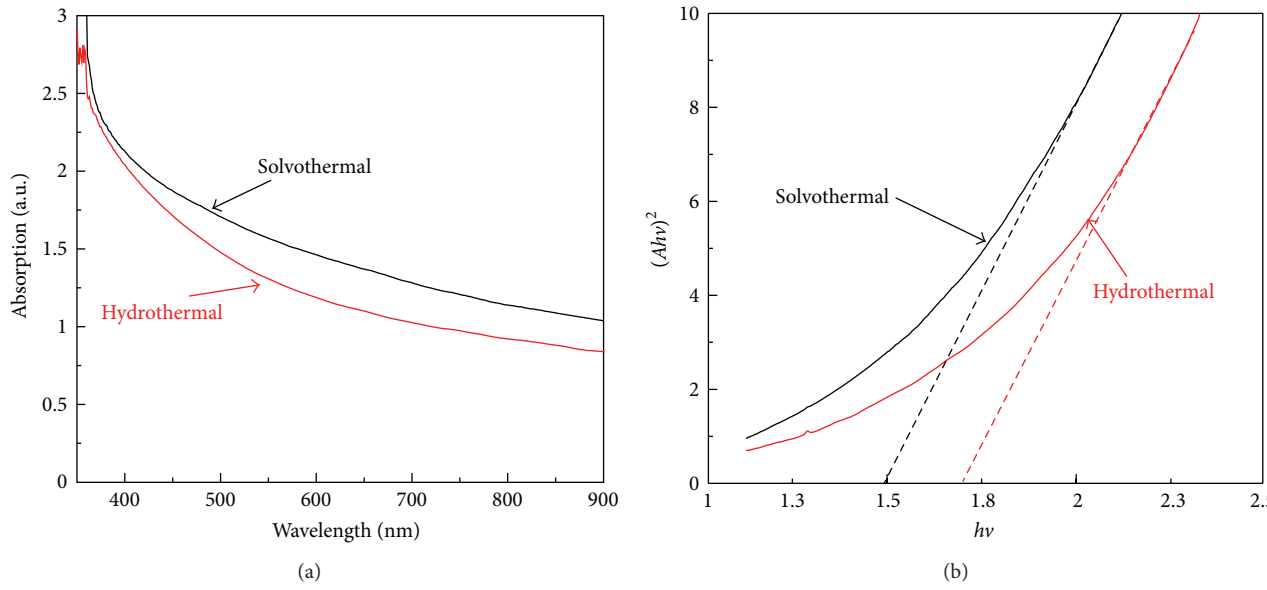

FIGURE 5: (a) Absorbance spectra of as-synthesized CZTS nanoparticles, and (b) $(Ahv)^2$ versus hv curve.

absorbance for visible light. The particle size of these nanomaterials is approximately 4-5 nm, and some effect of quantum confinement was observed for these CZTS nanocrystals, due to which an enhanced band gap of 1.7 eV was observed as compared to the bulk band gap of 1.45–1.5 eV reported for CZTS material. The solvothermally synthesized powder did not show any quantum confinement effect.

To propose the growth mechanism, we will first consider the reactions happening to yield CZTS powder. With the increase in temperature and stirring, metal ions are complexed with thiourea. (Thiourea in solution forms metal-thiourea complexes.) On hydrothermal heating, thiourea decomposes to give hydrogen sulfide (H_2S) as follows:

$$NH_2CSNH_2 + 2H_2O \longrightarrow 2NH_3 + H_2S + CO_2 \quad (1)$$

H_2S, produced in this way, reacts with different metal ions, to form CZTS compound. Thiourea plays two important roles in the formation of sulfides. First, it acts as a complexing reagent by forming metal-thiourea ligands, and second it acts as the source of sulfur after the breaking of C=S double bond by the strong nucleophilic substitution of the oxygen atoms in H_2O molecules [31]. The metal-thiourea ligands serves as a reservoir of metal ions and regulate the nucleation rate by the slow release of ions into solution. When the reactants were heated, the released S_2^- combined with the metal ions and precipitation of sulfides occurred due to the stronger coordination capability between metal ions and S_2^-. Because of the excess of thiourea, the metal atoms on the surface of the CZTS nanocrystallites formed could coordinate with excess thiourea and thus greatly restrict the growth of CZTS nanocrystallites. Due to this, hydrothermally synthesized CZTS is of smaller size as compared to solvothermally synthesized CZTS. Thus, both, the formation of metal-thiourea ligands and the gradual release of S_2^-, can control the nucleation and aggregation of CZTS nanocrystallites, leading to the large-scale harvesting of monodispersed nanocrystalline particles.

4. Conclusions

A simple and relatively safe approach of hydrothermal synthesis of the quaternary semiconductor Cu_2ZnSnS_4 (CZTS) nanoparticles was used. Nearly spherical nanoparticles of approximately 4-5 nm diameter were obtained without using any expensive vacuum facilities or high temperature annealing. The elemental analysis of the synthesized CZTS particles, performed by XRF, agreed well with the theoretical value of 2 : 1 : 1 : 4. The highly crystalline nature of the CZTS nanoparticles was confirmed by the X-ray diffraction and high-resolution TEM analysis. The appearance of the strongest Raman peak at 337.5 cm^{-1} in the Raman spectrum leaves no doubt about the formation of pure CZTS nanoparticles. An intercomparative study with solvothermal synthesis revealed that the hydrothermal process is far better in terms of being cheaper, easier, and environmentally green process. As-synthesized nanoparticles using solvothermal route produced mixed phase nanoparticles, which convert to pure CZTS only after annealing. The UV-Vis absorption spectrum exhibited broad absorption in the visible region. The band gap was estimated to be 1.7 eV which shows the quantum confinement effect in such small sized nanoparticles. The observation of such small sized nanoparticles using such a simple, greener, and inexpensive method is quite advantageous in the respect that hydrothermal synthesis route is well known for its large scale synthesis. There is no need for any capping agent to control the size, which is difficult and cumbersome to remove afterwards for most of the applications example for charge transfer among particles to take place.

Conflict of Interests

The authors declare that they have no conflict of interests.

Acknowledgments

The authors are thankful to (Technologies and Products for Solar Energy Utilization through Networks) (TAPSUN) program (NWP-54 Project) from CSIR for financial support. One of the authors (Shri kant Verma) is obliged to Professor R. C. Budhani (DNPL), for the kind permission for his project. The authors are obliged for the valuable discussion and suggestions given by Dr. Asit Patra. They are also thankful to Dr. N. Vijayan for XRD measurements, Mr. K. N. Sood, and SEM and TEM investigations.

References

[1] T. Wada, S. Nakamura, and T. Maeda, "Ternary and multinary Cu-chalcogenide photovoltaic materials from $CuInSe_2$ to Cu_2ZnSnS_4 and other compounds," *Progress in Photovoltaics*, vol. 20, no. 5, pp. 520–525, 2012.

[2] P. Jackson, D. Hariskos, E. Lotter et al., "New world record efficiency for $Cu(In,Ga)Se_2$ thin-film solar cells beyond 20%," *Progress in Photovoltaics*, vol. 19, no. 7, pp. 894–897, 2011.

[3] H. Katagiri, K. Jimbo, W. S. Maw et al., "Development of CZTS-based thin film solar cells," *Thin Solid Films*, vol. 517, no. 7, pp. 2455–2460, 2009.

[4] E. H. Sargent, "Infrared photovoltaics made by solution processing," *Nature Photonics*, vol. 3, no. 6, pp. 325–331, 2009.

[5] K. Tanaka, M. Oonuki, N. Moritake, and H. Uchiki, "Cu_2ZnSnS_4 thin film solar cells prepared by non-vacuum processing," *Solar Energy Materials and Solar Cells*, vol. 93, no. 5, pp. 583–587, 2009.

[6] H. Wang, "Progress in thin film solar cells based on Cu_2ZnSnS_4," *International Journal of Photoenergy*, vol. 2011, Article ID 801292, 10 pages, 2011.

[7] K. Ramaswamy, M. A. Malik, and P. O. Brien, "Routes to copper zinc tin sulfide Cu_2ZnSnS_4 a potential material for solar cells," *Chemical Communications*, vol. 48, pp. 5703–5714, 2012.

[8] T. K. Todorov, J. Tang, S. Bag et al., "Beyond 11% efficiency: characteristics of state of the art $Cu_2ZnSn(S, Se)_4$ solar cells," *Advanced Energy Materials*, vol. 3, no. 1, pp. 34–38.

[9] Q. Guo, G. M. Ford, W.-C. Yang et al., "Fabrication of 7.2% efficient CZTSSe solar cells using CZTS nanocrystals," *Journal of the American Chemical Society*, vol. 132, no. 49, pp. 17384–17386, 2010.

[10] B. Shin, O. Gunawan, Y. Zhu, N. A. Bojarczuk, S. J. Chey, and S. Guha, "Thin film solar cell with 8.4% power conversion efficiency using an earth-abundant Cu_2ZnSnS_4 absorber," *Progress in Photovoltaics*, vol. 21, no. 1, pp. 72–76, 2013.

[11] S. E. Habas, H. A. S. Platt, M. F. A. M. Van Hest, and D. S. Ginley, "Low-cost inorganic solar cells: from ink to printed device," *Chemical Reviews*, vol. 110, no. 11, pp. 6571–6594, 2010.

[12] A. Khare, A. W. Wills, L. M. Ammerman, D. J. Norris, and E. S. Aydil, "Size control and quantum confinement in Cu_2ZnSnS_4 nanocrystals," *Chemical Communications*, vol. 47, no. 42, pp. 11721–11723, 2011.

[13] C. Steinhagen, M. G. Panthani, V. Akhavan, B. Goodfellow, B. Koo, and B. A. Korgel, "Synthesis of Cu_2ZnSnS_4 nanocrystals for use in low-cost photovoltaics," *Journal of the American Chemical Society*, vol. 131, no. 35, pp. 12554–12555, 2009.

[14] Q. J. Guo, H. W. Hillhouse, and R. Agrawal, "Synthesis of Cu_2ZnSnS_4 nanocrystal ink and its use for solar cells," *Journal of the American Chemical Society*, vol. 131, no. 33, pp. 11672–11673, 2009.

[15] M. Rajamathi and R. Seshadri, "Oxide and chalcogenide nanoparticles from hydrothermal/solvothermal reactions," *Current Opinion in Solid State and Materials Science*, vol. 6, no. 4, pp. 337–345, 2002.

[16] H. Zhang, X. Ma, Y. Ji, J. Xu, and D. Yang, "Single crystalline CdS nanorods fabricated by a novel hydrothermal method," *Chemical Physics Letters*, vol. 377, no. 5-6, pp. 654–657, 2003.

[17] L. Wang, J. Dai, X. Liu, Z. Zhu, X. Huang, and P. Wu, "Morphology-controlling synthesis of ZnS through a hydrothermal/solvthermal method," *Ceramics International*, vol. 38, no. 3, pp. 1873–1878, 2012.

[18] H. Gong, H. Huang, M. Wang, and K. Liu, "Characterization and growth mechanism of ZnSe microspheres prepared by hydrothermal synthesis," *Ceramics International*, vol. 33, no. 7, pp. 1381–1384, 2007.

[19] Q. Lu, J. Hu, K. Tang, Y. Qian, G. Zhou, and X. Liu, "Synthesis of nanocrystalline $CuMS_2$ (M = In or Ga) through a solvothermal process," *Inorganic Chemistry*, vol. 39, no. 7, pp. 1606–1607, 2000.

[20] J. Chang, J. E. Han, and D.-Y. Jung, "Solvothermal synthesis of copper indium diselenide in toluene," *Bulletin of the Korean Chemical Society*, vol. 32, no. 2, pp. 434–438, 2011.

[21] J. Madarász, P. Bombicz, M. Okuya, and S. Kaneko, "Thermal decomposition of thiourea complexes of Cu(I), Zn(II), and Sn(II) chlorides as precursors for the spray pyrolysis deposition of sulfide thin films," *Solid State Ionics*, vol. 141-142, pp. 439–446, 2001.

[22] C. Wang, C. Cheng, Y. Cao, W. Fang, L. Zhao, and X. Xu, "Synthesis of Cu_2ZnSnS_4 nanocrystallines by a hydrothermal route," *Japanese Journal of Applied Physics*, vol. 50, no. 6, Article ID 065003, 2011.

[23] M. Cao and Y. Shen, "A mild solvothermal route to kesterite quaternary Cu_2ZnSnS_4 nanoparticles," *Journal of Crystal Growth*, vol. 318, no. 1, pp. 1117–1120, 2011.

[24] H. Jiang, P. Dai, Z. Feng, W. Fan, and J. Zhan, "Phase selective synthesis of metastable orthorhombic Cu_2ZnSnS_4 ," *Journal of Materials Chemistry*, vol. 22, no. 15, pp. 7502–7506, 2012.

[25] Y.-F. Du, W.-H. Zhou, Y.-L. Zhou et al., "Solvothermal synthesis and characterization of quaternary $Cu_2ZnSnSe_4$ particles," *Materials Science in Semiconductor Processing*, vol. 5, pp. 214–217, 2012.

[26] L. Shi and Q. Li, "Thickness tunable $Cu_2ZnSnSe_4$ nanosheets," *CrystEngComm*, vol. 13, no. 21, pp. 6507–6510, 2011.

[27] Y.-L. Zhou, W.-H. Zhou, Y.-F. Du, M. Li, and S.-X. Wu, "Sphere-like kesterite Cu_2ZnSnS_4 nanoparticles synthesized by a facile solvothermal method," *Materials Letters*, vol. 65, no. 11, pp. 1535–1537, 2011.

[28] O. Zaberca, A. Gillorin, B. Durand, and J. Y. Chane-Ching, "A general route to the synthesis of surfactant-free, solvent-dispersible ternary and quaternary chalcogenide nanocrystals," *Journal of Materials Chemistry*, vol. 21, no. 18, pp. 6483–6486, 2011.

[29] Y.-L. Zhou, W.-H. Zhou, M. Li, Y.-F. Du, and S.-X. Wu, "Hierarchical Cu_2ZnSnS_4 particles for a low-cost solar cell: morphology control and growth mechanism," *Journal of Physical Chemistry C*, vol. 115, no. 40, pp. 19632–19639, 2011.

[30] Y. Wang and H. Gong, "Low temperature synthesized quaternary chalcogenide Cu_2ZnSnS_4 from nano-crystallite binary sulfides," *Journal of the Electrochemical Society*, vol. 158, no. 8, pp. H800–H803, 2011.

[31] M. Grossberg, J. Krustok, J. Raudoja, K. Timmo, M. Altosaar, and T. Raadik, "Photoluminescence and Raman study of $Cu_2ZnSn(Se_xS_{1-X})_4$ monograins for photovoltaic applications," *Thin Solid Films*, vol. 519, no. 21, pp. 7403–7406, 2011.